

Growth of nanotextured thin films of GaInAsP and GaInAsSbBi solid solutions on GaP substrates by pulsed laser deposition

Alexander S. Pashchenko^{1,2,a,b}, Oleg V. Devitsky^{1,2,c}, Leonid S. Lunin^{1,2}, Marina L. Lunina¹, Olga S. Pashchenko¹, Eleonora M. Danilina¹

¹Federal Research Center Southern Scientific Center of the Russian Academy of Sciences, Rostov-on-Don, Russia

²North Caucasian Federal University, Stavropol, Russia

^asemicondlab@ya.ru, ^bas.pashchenko@gmail.com, ^cv2517@rambler.ru

Corresponding author: Alexander S. Pashchenko, semicondlab@ya.ru, as.pashchenko@gmail.com

PACS 68.35.Ct, 68.55.Jk, 81.15.-z, 81.15.Cd

ABSTRACT GaInAsP and GaInAsSbBi solid solutions were grown on GaP (111) substrates by pulsed laser deposition using a laser fluence of 2.3 J/cm². Energy Dispersive X-ray microanalysis, atomic force microscopy, and Raman spectroscopy were used for analysis of the elemental composition and study of the surface morphology and chemical bonds of the obtained solid solutions. It was found that at constant growth temperature and the fluence of 2.3 J/cm², the elemental composition of the film has a significant effect on the growth kinetics. Surface-active elements (Sb and Bi) in the composition of the solid solution lead to a change in the surface diffusion of In and Ga, which is accompanied by a decrease in roughness. It was established that the films growth in the Volmer–Weber mode. The grown films are nanotextured with a predominant orientation in the direction of growth (111).

KEYWORDS pulsed laser deposition, solid solutions, GaP, semiconductors, III–V compounds

ACKNOWLEDGEMENTS This work was funded as part of a state order to the Southern Scientific Centre of the Russian Academy of Sciences, projects No. 122020100254-3 (studies of chemical composition and morphology) and No. 122020100326-7 (Raman studies). The growth of experimental samples was carried out using the resources of Center for Collective Use of North Caucasus Federal University and with the financial support of the Ministry of Education and Science of Russia, the unique identifier of the project is RF-2296.61321X0029 (agreement No. 075-15-2021-687).

The authors express their gratitude to the North Caucasian Federal University for their assistance in the framework of the competition for supporting projects of scientific groups and individual scientists of the university.

FOR CITATION Pashchenko A.S., Devitsky O.V., Lunin L.S., Lunina M.L., Pashchenko O.S., Danilina E.M. Growth of nanotextured thin films of GaInAsP and GaInAsSbBi solid solutions on GaP substrates by pulsed laser deposition. *Nanosystems: Phys. Chem. Math.*, 2023, **14** (5), 601–605.

1. Introduction

Pulsed laser deposition (PLD) is a promising and rapidly developing method for obtaining multicomponent compounds [1–3]. The advantages of PLD over other methods of physical deposition are the possibility of controlling the film stoichiometry, lowering the substrate temperature for growing thin III–V films, and the discrete flow of a substance from the target to the substrate in the time intervals between laser pulses. The advantage of the method is its relative simplicity of equipment, high purity of the deposited layers, and preservation of the stoichiometry of the chemical composition of a layer and a sputtered target [3, 4]. During PLD at the laser fluence of less than 2 J/cm², an erosion-plasma plume forms a spot beam, due to which the expansion diagram of some target components, especially volatile ones, for example, As, P, Sb. In PLD at the laser fluence of more than 2 J/cm², the uniformity of the expansion of the target components increases, but the growth kinetics and properties of the grown films change simultaneously [4]. As applied to III–V and CIGS semiconductor solid solutions, if the target contains more than one group III metal, then droplets can be formed on the surface [5, 6], the morphology deteriorates, and the layer stoichiometry is violated [7]. To understand these processes under PLD conditions, in this work, we study the properties of films grown with the laser fluence of 2.3 J/cm².

The objects of study were Ga_xIn_{1-x}As_yP_{1-y} and Ga_xIn_{1-x}As_{1-y-z}Sb_yBi_z solid solutions deposited on GaP substrates. The solid solutions consisting of two group III metals and three highly volatile group V metalloids were selected based on the indicated difficulties in PLD, as well as on the relevance of their practical use for growing optoelectronic heterostructures in the visible [8] and infrared [9] ranges. The study of solid solutions with Bi and Sb is topical due to the discovery of the effect of valence band anticrossing [10], which significantly affects the optoelectronic properties of dilute

semiconductors. The object of this work is to grow $\text{Ga}_x\text{In}_{1-x}\text{As}_y\text{P}_{1-y}$ and $\text{Ga}_x\text{In}_{1-x}\text{As}_{1-y-z}\text{Sb}_y\text{Bi}_z$ solid solutions on GaP (111) substrates by PLD at the laser fluence of 2.3 J/cm^2 and study the morphology, chemical composition, and chemical bonds in them.

2. Methods and experiments

PLD of $\text{Ga}_x\text{In}_{1-x}\text{As}_y\text{P}_{1-y}$ and $\text{Ga}_x\text{In}_{1-x}\text{As}_{1-y-z}\text{Sb}_y\text{Bi}_z$ solid solutions was carried out using an AYG:Nd³⁺ laser (LS-2134Y) with a wavelength of 532 nm (second harmonic). For sputtering, we used targets with the calculated composition $\text{Ga}_{0.84}\text{In}_{0.16}\text{As}_{0.68}\text{P}_{0.32}$ and $\text{Ga}_{0.85}\text{In}_{0.15}\text{Sb}_{0.1}\text{As}_{0.8}\text{Bi}_{0.1}$. The deposition was carried out on n-GaP (111) substrates. The choice of the substrate with the (111) orientation is due to the specifics of growth due to the polarity of Group III–V solid solutions, as well as the closeness of the lattice parameters of GaP and Si. We used the classical PLD method. The deposition time for all samples was 60 min, and the background pressure in the chamber was 10^{-4} Pa. The distance from the target to the substrate was 70 mm. Growth was carried out at a temperature of 450 °C, a laser fluence $F = 2.3 \text{ J/cm}^2$, pulse duration time 10 ns, pulse-recurrence frequency 15 Hz.

The chemical composition was determined by Energy Dispersive X-ray microanalysis (EDX) using an INCAx-sight attachment (Oxford Instruments, UK) on a Carl Zeiss Evo 40 microscope with a beam energy of 8 keV to reduce the signal from the substrate. The film thickness was determined from the cleavages of the structures on a Carl Zeiss Evo 40 microscope. The study of the morphology and root-mean-square (RMS) roughness of the films was carried out on an atomic force microscope (AFM) “NTEGRA Academia” (NT-MDT SI, Russia). Scanning was carried out in a tapping mode. An NS15 silicon cantilever with a resonant frequency of 373.35 kHz and a curvature radius of 10 nm was used as a probe. The scanning speed varied in the range of 0.6 – 1 Hz depending on the surface topography. Line-scan direction is forward. The scanning area is $1 \times 1 \mu\text{m}^2$. AFM images were processed using the Gwyddion program [11]. The filtering included standard operations of subtracting the surface of the 3rd order, removing steps in the X direction, and removing scratches. The root-mean-square roughness parameter S_q was estimated for the entire scan area as an estimated value of the surface roughness. The study of chemical bonds in the obtained films was carried out by Raman spectroscopy on an inVia Raman Microscope spectrometer (Renishaw, UK) with an excitation wavelength of 514 nm at room temperature.

3. Results and discussions

At the first stage, the elemental analysis was carried out by the EDS (Fig. 1). In the spectra in Fig. 1, all the chemical elements of $\text{Ga}_x\text{In}_{1-x}\text{As}_y\text{P}_{1-y}$ (Fig. 1a) and $\text{Ga}_x\text{In}_{1-x}\text{As}_{1-y-z}\text{Sb}_y\text{Bi}_z$ (Fig. 1b) solid solutions were presented. The features of the measured EDX spectra are the high intensity of the Ga and P peaks and the low intensities of the Bi, Sb, and As peaks.

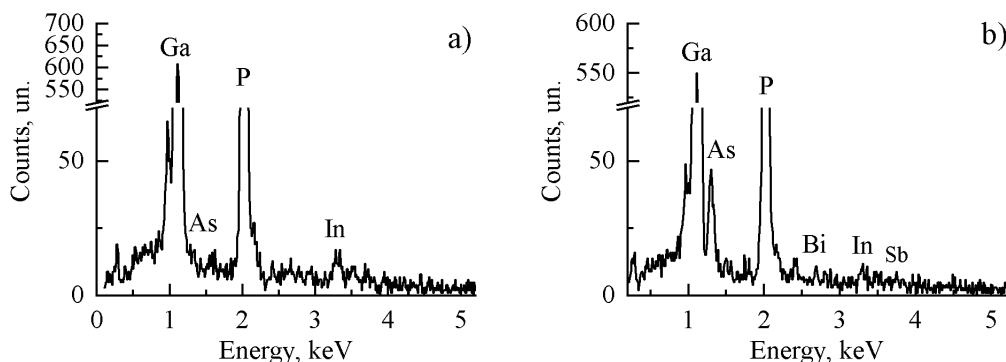


FIG. 1. EDX spectra of elemental analysis of solid solutions on n-GaP (111) substrates: a) GaInAsP; b) GaInAsSbBi

Estimation of the atomic concentration of the solid solution elements gave one the following results: for $\text{Ga}_x\text{In}_{1-x}\text{As}_y\text{P}_{1-y}$: Ga – 46.32 at.%; In – 2.66 at.%; As – 0.56 at.%, P – 50.45 at.%; for $\text{Ga}_x\text{In}_{1-x}\text{As}_{1-y-z}\text{Sb}_y\text{Bi}_z$: Ga – 47.26 at.%; In – 1.93 at.%; As – 21.31 at.%, Sb – 1.32 at.%; Bi – 0.89 at.%; P – 29.46 at.%. The phosphorus in the EDX spectrum (Fig. 1b) is due to its presence in the substrate and the small film thickness. This factor also introduces an error in determining the concentration of elements of group V. Nevertheless, for qualitative elemental analysis, the EDX method gives reliable results. The thickness of the grown films was determined from the cleavages of the heterostructure: GaInAsP – 223 nm; GaInAsSbBi – 152 nm. It can be seen that the growth film kinetics increases significantly.

Figure 2a shows the results of study of the morphology of the grown films by the AFM. In the case of the $\text{Ga}_x\text{In}_{1-x}\text{As}_y\text{P}_{1-y}$ solid solution (Fig. 2a), the developed relief pattern is on the film surface. The height difference is 43 nm, and the RMS roughness $S_q = 5.2$ nm. In the case of the GaInAsSbBi solid solution (Fig. 2b), the maximum height difference reaches 23 nm with the RMS roughness $S_q = 2.8$ nm. A distinctive feature of the $\text{Ga}_x\text{In}_{1-x}\text{As}_{1-y-z}\text{Sb}_y\text{Bi}_z$

film is the larger grain size with a smoother surface than in the case of the GaInAsP film with a highly developed surface relief pattern. In Fig. 2a the surface topography is due to chaotic grain boundaries, which are antiphase boundaries. Only some grains have plateaus on the surface oriented in the (111) plane. At the same time, the grain boundaries in the $\text{Ga}_x\text{In}_{1-x}\text{As}_{1-y-z}\text{Sb}_y\text{Bi}_z$ film (Fig. 2b) appear as dislocations along certain directions, and to a greater extent have lateral faceting along the (110) planes, while plateaus in the growth direction are predominantly orientation in the (111) plane, i.e. the $\text{Ga}_x\text{In}_{1-x}\text{As}_{1-y-z}\text{Sb}_y\text{Bi}_z$ film is nanotextured. It can be seen that in the case of the film in Fig. 2b, a large surface area is represented by hillocks with a plateau at the top, rather than pits, which also reveals itself in a lower RMS roughness S_q .

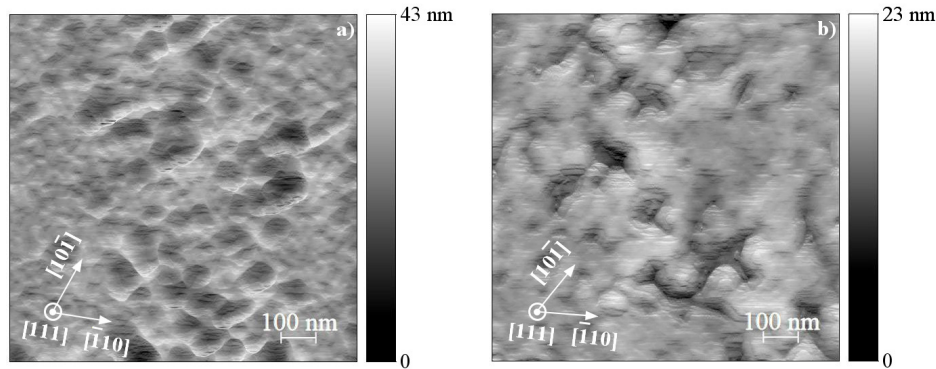


FIG. 2. AFM images ($1 \times 1 \mu\text{m}$) of solid solution morphology on n-GaP (111) substrates: a) GaInAsP; b) GaInAsSbBi

The AFM analysis shows that the selected solid solutions grow at different rates due to different surface diffusion at the same growth temperature of 450°C and laser fluence $F = 2.3 \text{ J/cm}^2$. Therefore, under PLD conditions, the growth kinetics is significantly affected by the elemental composition of the film. The larger grain size in the $\text{Ga}_x\text{In}_{1-x}\text{As}_{1-y-z}\text{Sb}_y\text{Bi}_z$ film is explained by the presence of Bi in its composition. It is known that Bi has a high surface diffusion and exhibits a strong surfactant effect [12], due to which it leads to a significant change in the diffusion of indium. These factors explain the larger grain size in Fig. 2b. Based on the AFM results, it can be concluded that the growth of thin films occurs through the nucleation of 3D islands, and then their coalescence occurs; the mode of epitaxial growth according to Volmer–Weber is implemented. Note that outside researchers also observed a similar growth when growing strongly mismatched group III–V heterostructures using other methods [13–15].

Raman spectra were measured to study the chemical bonds between the elements of the solid solution (Fig. 3). Table 1 summarizes the results of the measured frequencies of the phonon optical modes of the components of solid solutions and their values published in the literature references.

From the features of the measured spectra (Fig. 3), one can distinguish the dominance of the GaP LO (404.46 cm^{-1}) and TO (364 cm^{-1}) modes for both solid solutions, due to the small thickness of the films and the penetration of laser radiation into the substrate GaP, as well as the mode shift of GaAs, GaSb, InAs, and InSb in the region ($200 - 300 \text{ cm}^{-1}$), compared with the literature data (Table 1). In the case of the $\text{Ga}_x\text{In}_{1-x}\text{As}_y\text{P}_{1-y}$ solid solution (Fig. 3a), the peaks of InP LO (339.1 cm^{-1}) and TO (313.16 cm^{-1}) have weak intensities, which is due to its low concentration in the layer and the predominance of indirect-gap optical transitions [13].

Another feature of the Raman spectrum in Fig. 3a is the predominance of GaAs TO modes over GaAs LO in intensity, as well as their low intensity compared to those in $\text{Ga}_x\text{In}_{1-x}\text{As}_{1-y-z}\text{Sb}_y\text{Bi}_z$ solid solution. In the $\text{Ga}_x\text{In}_{1-x}\text{As}_{1-y-z}\text{Sb}_y\text{Bi}_z$ solid solution (Fig. 3b), the GaAs LO mode dominates over the GaAs TO mode in intensity with their simultaneous shift to lower wavenumbers (Table 1). This effect is explained by higher As concentration in the $\text{Ga}_x\text{In}_{1-x}\text{As}_{1-y-z}\text{Sb}_y\text{Bi}_z$ film compared to $\text{Ga}_x\text{In}_{1-x}\text{As}_y\text{P}_{1-y}$ (Fig. 1). The shift of these modes is due to the relaxation mechanisms in the film and the presence of dislocations (Fig. 2b). We associate the broad peak at 208.66 cm^{-1} with the GaBi LO mode, whose position is close to the theoretical 205 cm^{-1} [16]. The mode shift of InAs, InSb, GaSb, GaBi, and InBi is explained by the difference in the concentrations of Sb, Bi, As and the shift of electron densities during the formation of chemical bonds In–As, In–Sb, In–Bi, Ga–Sb, Ga–Bi. These factors indicate a violation of the selection rule for the zinc blende lattice, which is expressed in the mixing of phonon modes (InBi + InSb) in the range of $150 - 200 \text{ cm}^{-1}$ due to disordering of the elements (disturbance of long-range order) of the solid solution.

4. Conclusion

In conclusion, we note that nanotextured $\text{Ga}_x\text{In}_{1-x}\text{As}_y\text{P}_{1-y}$ and $\text{Ga}_x\text{In}_{1-x}\text{As}_{1-y-z}\text{Sb}_y\text{Bi}_z$ solid solutions with a laser fluence of 2.3 J/cm^2 were grown by PLD. It is shown that in the case of PLD with a high fluence, the stoichiometry of the composition of solid solutions is disturbed. It is established that at constant growth temperature and the fluence

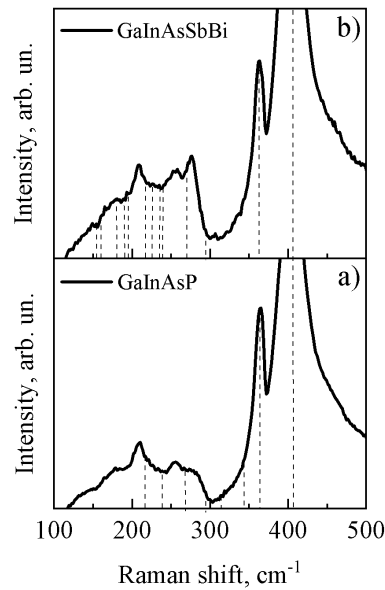


FIG. 3. Raman shift spectra of solid solutions on n-GaP (111) substrates: a) GaInAsP; b) GaInAsSbBi. Dashed lines indicate the frequencies of phonon modes from the literature (Table 1)

TABLE 1. Phonon frequencies of group III–V binary components constituting GaInAsP and GaInAsSbBi alloys

Binary component of a solid solution	Known phonon mode frequencies		Measured frequencies of phonon modes in the GaInAsP solid solution		Measured frequencies of phonon modes in the GaInAsSbBi solid solution	
	LO, cm ⁻¹	TO, cm ⁻¹	LO, cm ⁻¹	TO, cm ⁻¹	LO, cm ⁻¹	TO, cm ⁻¹
GaP	402 [16]	363 [16]	404.46	364.95	—	—
GaAs	292 [17]	268 [11]	281.93	255.84	276.73	257.58
InP	344 [18]	312 [18]	339.1	313.16	—	—
InAs	238.8 [19]	217.3 [19]	233.15	210.42	252.35	220.92
GaSb	236 [17]	226 [17]	—	—	234.90	226.16
InSb	190.8 [19]	179.8 [19]	—	—	192.88	180.59
InBi	161 [20]	155 [20]	—	—	161.24	154.19
GaBi	205 [21]	189 [20]	—	—	208.66	189.37

under PLD conditions, the elemental composition of the film has a significant effect on the growth kinetics. The surface-active elements (Sb and Bi) in the composition of the solid solution lead to a change in the surface diffusion of In and Ga. It is established that the growth of films occurs according to the Volmer–Weber mode. The AFM results show that the relaxation of stresses caused by the mismatch of the crystal lattices of $\text{Ga}_x\text{In}_{1-x}\text{As}_y\text{P}_{1-y}$ and $\text{Ga}_x\text{In}_{1-x}\text{As}_{1-y-z}\text{Sb}_y\text{Bi}_z$ and the GaP substrate occurs through plastic mechanisms and a change in roughness, which manifests itself in the formation of grains in the texture of the grown thin films. To improve the structural properties of the films, we plan to use GaAs buffer layers for the growth of $\text{Ga}_x\text{In}_{1-x}\text{As}_y\text{P}_{1-y}$ and $\text{Ga}_x\text{In}_{1-x}\text{As}_{1-y-z}\text{Sb}_y\text{Bi}_z$ solid solutions.

References

- [1] Ogugua S.N., Ntwaeaborwa O.M., Swart H.C. Latest Development on Pulsed Laser Deposited Thin Films for Advanced Luminescence Applications. *Coatings*, 2020, **10** (11), 1078.
- [2] Li G., Wang W., Yang W., Wang H. Epitaxial growth of group III-nitride films by pulsed laser deposition and their use in the development of LED devices. *Surface Science Reports*, 2015, **70** (3), P. 380–423.
- [3] Vanalakar S.A., Agawane G.L., Shin S.W., Suryawanshi M.P., Gurav K.V., Jeon K.S., Patil P.S., Jeong C.W., Kim J.Y., Kim J.H. A review on pulsed laser deposited CZTS thin films for solar cell applications. *J. of Alloys and Compounds*, 2015, **619**, P. 109–121.

- [4] Ettlinger R.B., Cazzaniga A., Canulescu S., Pryds N., Schou J. Pulsed laser deposition from ZnS and Cu₂SnS₃ multicomponent targets. *Applied Surface Science*, 2015, **336**, P. 385–390.
- [5] Pashchenko A.S., Devitsky O.V., Lunin L.S., Kasyanov I.V., Pashchenko O.S., Nikulin D.A. Structure and morphology of GaInAsP solid solutions on GaAs substrates grown by pulsed laser deposition. *Thin Solid Films*, 2022, **743**, 139064.
- [6] Chen S.C., Hsieh D.H., Jiang H., Liao Y.K., Lai F.I., Chen C.H., Luo C.W., Juang J.Y., Chueh Y.L., Wu K.H., Kuo H.C. Growth and characterization of Cu(In,Ga)Se₂ thin films by nanosecond and femtosecond pulsed laser deposition. *Nanoscale Research Letters*, 2014, **9**, 280.
- [7] Pashchenko A.S., Devitsky O.V., Lunin L.S., Lunina M.L., Pashchenko O.S. Structural properties of GaInAsSbBi solid solutions grown on GaSb substrates. *Technical Physics Letters*, 2022, **48** (5), P. 52–55.
- [8] Oshima R., France R.M., Geisz J.F., Norman A.G., Steiner M.A. Growth of lattice-matched GaInAsP grown on vicinal GaAs(001) substrates within the miscibility gap for solar cells. *J. of Crystal Growth*, 2017, **458**, P. 1–7.
- [9] Carrasco R.A., Morath C.P., Logan J.V., Woller K.B., Grant P.C., Orozco H., Milosavljevic M.S., Johnson S.R., Balakrishnan G., Webster P.T. Photoluminescence and minority carrier lifetime of quinary GaInAsSbBi grown on GaSb by molecular beam epitaxy. *Applied Physics Letters*, 2022, **120** (3), 031102.
- [10] Alberi K., Wu J., Walukiewicz W., Yu K.M., Dubon O.D., Watkins S.P., Wang C.X., Liu X., Cho Y.-J., Furdyna J. Valence-band anticrossing in mismatched III–V semiconductor alloys. *Physical Review B*, 2007, **75**, 045203.
- [11] Nečas D., Klapetek P. Gwyddion: an open-source software for SPM data analysis. *Open Physics*, 2012, **10** (1), P. 181–188.
- [12] Zvonkov B.N., Karpovich I.A., Baidus N.V., Filatov D.O., Morozov S.V., Gushina Yu.Yu. Surfactant effect of bismuth in the MOVPE growth of the InAs quantum dots on GaAs. *Nanotechnology*, 2000, **11** (4), P. 221–226.
- [13] Devenyi G.A., Woo S.Y., Ghanad-Tavakoli S., Hughes R.A., Kleiman R.N., Botton G.A., Preston J.S. The role of vicinal silicon surfaces in the formation of epitaxial twins during the growth of III–V thin films. *J. of Applied Physics*, 2011, **110** (12), 124316.
- [14] Fang S.F., Adomi K., Iyer S., Morkoç H., Zabel H., Choi C., Otsuka N. Gallium arsenide and other compound semiconductors on silicon. *J. of Applied Physics*, 1990, **68** (7), R31–R58.
- [15] Kim Y.H., Noh Y.K., Kim M.D., Oh J.E., Chung K.S. Transmission electron microscopy study of the initial growth stage of GaSb grown on Si (001) substrate by molecular beam epitaxy method. *Thin Solid Films*, 2010, **518** (8), P. 2280–2284.
- [16] Gudovskikh A.S., Uvarov A.V., Morozov I.A., Baranov A.I., Kudryashov D.A., Zelentsov K.S., Bukatin A.S., Kotlyar K.P. Low temperature plasma enhanced deposition approach for fabrication of microcrystalline GaP/Si superlattice. *J. of Vacuum Science & Technology A*, 2018, **36** (2), 02D408.
- [17] Vorlíček V., Moiseev K.D., Mikhailova M.P., Yakovlev Yu.P., Hulicius E., Šimeček T. Raman Scattering Study of Type II GaInAsSb/InAs Heterostructures. *Crystal Research & Technology*, 2002, **37** (2–3), P. 259–267.
- [18] Bedel E., Landa G., Carles R., Redoules J.P., Renucci J.B. Raman investigation of the InP lattice dynamics. *J. of Physics C: Solid State Physics*, 1986, **19**, 1471.
- [19] Frost F., Lippold G., Schindler A., Bigl F. Ion beam etching induced structural and electronic modification of InAs and InSb surfaces studied by Raman spectroscopy. *J. of Applied Physics*, 1999, **85** (12), P. 8378–8385.
- [20] Verma P., Oe K., Yamada M., Harima H., Herms M., Irmer G. Raman studies on GaAs_{1-x}Bi_x and InAs_{1-x}Bi_x. *J. of Applied Physics*, 2001, **89** (3), P. 1657–1663.
- [21] Yue L., Wang P., Wang K., Wu X., Pan W., Li Y., Song Y., Gu Y., Gong Q., Wang Sh., Ning J., Xu Sh. Novel InGaPBi single crystal grown by molecular beam epitaxy. *Applied Physics Express*, 2015, **8** (4), 041201.

Submitted 3 July 2023; revised 9 August 2023; accepted 20 August 2023

Information about the authors:

Alexander S. Pashchenko – Federal Research Center Southern Scientific Center of the Russian Academy of Sciences, Chekhov Ave., 41, Rostov-on-Don, 344006, Russia; North Caucasian Federal University, Pushkina st., 1, Stavropol, 355017, Russia; ORCID 0000-0002-7976-9597; semicondlab@ya.ru, as.pashchenko@gmail.com

Oleg V. Devitsky – Federal Research Center Southern Scientific Center of the Russian Academy of Sciences, Chekhov Ave., 41, Rostov-on-Don, 344006, Russia; North Caucasian Federal University, Pushkina st., 1, Stavropol, 355017, Russia; ORCID 0000-0003-3153-696X; v2517@rambler.ru

Leonid S. Lunin – Federal Research Center Southern Scientific Center of the Russian Academy of Sciences, Chekhov Ave., 41, Rostov-on-Don, 344006, Russia; North Caucasian Federal University, Pushkina st., 1, Stavropol, 355017, Russia; ORCID 0000-0002-5534-9694; lunin_LS@mail.ru

Marina L. Lunina – Federal Research Center Southern Scientific Center of the Russian Academy of Sciences, Chekhov Ave., 41, Rostov-on-Don, 344006, Russia; ORCID 0009-0004-5761-3999; MarinaSchaz@rambler.ru

Olga S. Pashchenko – Federal Research Center Southern Scientific Center of the Russian Academy of Sciences, Chekhov Ave., 41, Rostov-on-Don, 344006, Russia; ORCID 0000-0003-3698-1835; paschenko.o.s@mail.ru

Eleonora M. Danilina – Federal Research Center Southern Scientific Center of the Russian Academy of Sciences, Chekhov Ave., 41, Rostov-on-Don, 344006, Russia; ORCID 0000-0001-6232-3217; el.m.danilina@gmail.com

Conflict of interest: the authors declare no conflict of interest.